

# A Modified Turbulent Model for the Supercritical Water Flows in the Vertical Upward Channels

Huirui Han, Chao Zhang\*

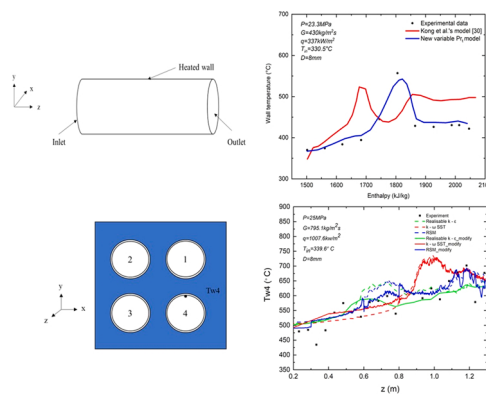
Department of Mechanical &amp; Materials Engineering, Western University, 1151 Richmond Street, London, ON N6A 5B9, Canada



## HIGHLIGHTS

- The capability of the existing turbulence models in the prediction of the supercritical fluid flow was assessed.
- A new variable  $Pr_t$  model was proposed.
- The proposed  $Pr_t$  model can improve the accuracy of the prediction for the supercritical fluid flow and heat transfer.
- The performance of the proposed  $Pr_t$  model was assessed under different operating conditions.

## GRAPHICAL ABSTRACT



## ARTICLE INFO

### Keywords:

SCWR  
Numerical simulation  
Modified turbulent model  
Wall temperature  
Prandtl number

## ABSTRACT

The supercritical water undergoes drastic changes in the thermal physical properties near the pseudo-critical point. It is necessary to evaluate whether the conventional turbulent models could successfully capture the wall temperature variations. In this study, the heat transfer of the supercritical water in the vertical tube and multiple fuel rods channel is numerically investigated using different turbulent models. The numerical results are compared with the experimental data. The comparisons indicate that the realisable  $k - \varepsilon$  model,  $k - \omega$  SST model, and the Reynolds stress model generally give a better agreement with the experimental data on the predictions of the wall temperatures. A new variable turbulent Prandtl model is proposed. Selected better performance turbulent models coupled with the proposed turbulent Prandtl model are assessed. The modified turbulent model shows a great improvement in the prediction of the wall temperatures, especially for the condition in a multiple fuel rods channel.

## 1. Introduction

The supercritical water-cooled reactor (SCWR) is one of the proposed

six Generation IV reactors [1]. The working fluid used as the coolant in the fuel bundle of the Canadian SCWR core is the supercritical water. The thermal physical properties of the supercritical water change dramatically near the pseudo-critical point (as shown in Fig. 1) [2]. The

\* Corresponding author.

E-mail addresses: [hhan55@uwo.ca](mailto:hhan55@uwo.ca) (H. Han), [cchang@eng.uwo.ca](mailto:cchang@eng.uwo.ca) (C. Zhang).

<b>Nomenclature</b>		$\sigma_k$	Turbulent Prandtl number for $k$
$c_p$	Specific heat, J/kg·K	$\sigma_\varepsilon$	Turbulent Prandtl number for $\varepsilon$
$D$	Diameter of a tube, m	$\sigma_\omega$	Turbulent Prandtl number for $\omega$
$g$	Gravitational acceleration, m/s <sup>2</sup>	$\omega$	Specific dissipation rate, 1/s
$G$	Mass flux, kg/m <sup>2</sup> s	<i>Subscripts</i>	
$k$	Turbulence kinetic energy, m <sup>2</sup> /s <sup>2</sup>	$cr$	Critical
$L$	Length, m	$in$	Inlet
$P$	Pressure, Pa	$m$	Mean
$Pr$	Prandtl number	$pc$	Pseudo-critical
$q$	Heat flux, W/m <sup>2</sup>	$t$	Turbulent
$T$	Temperature, °C	$w$	Wall
$u$	Velocity, m/s	<i>Acronyms</i>	
$y$	Distance from the wall, m	CFD	Computational Fluid Dynamics
$y^+$	Nondimensional distance from the wall, $y^+ = \frac{u_y y}{\nu}$	NHT	Normal Heat Transfer
$z$	Axial location, m	DHT	Deteriorate Heat transfer
<i>Greek Letters</i>		MAE	Mean of Absolute Error
$\alpha$	Thermal diffusivity, m <sup>2</sup> /s	RE	Relative Error
$\varepsilon$	Turbulence kinetic energy dissipation, m <sup>2</sup> /s <sup>3</sup>	RNG	Renormalization Group
$\mu$	Dynamic viscosity, Pa · s	RSM	Reynold Stress Model
$\nu$	Kinematic viscosity, m <sup>2</sup> /s	SCWR	Supercritical Water-Cooled Reactor
$\lambda$	Thermal conductivity, W/m · K	SD	Standard Deviation
$\rho$	Density of a fluid, kg/m <sup>3</sup>	SST	Shear Stress Transport

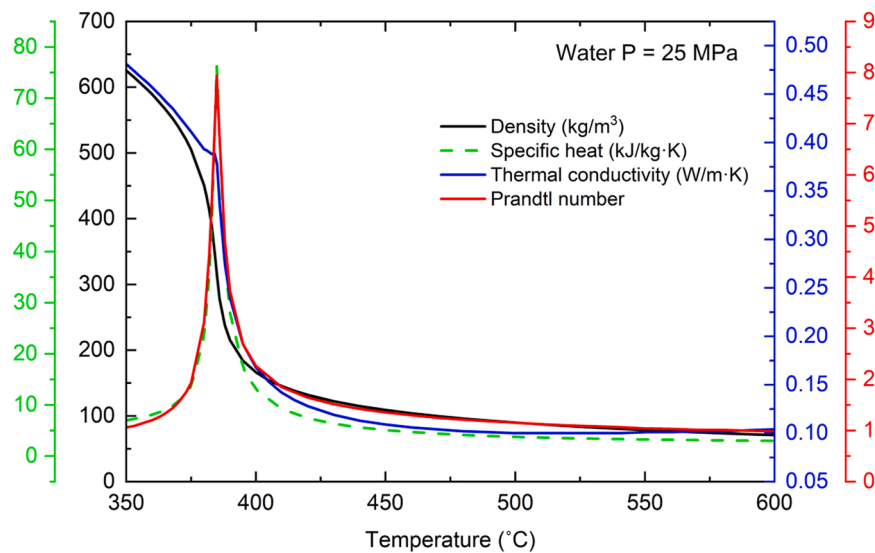


**Fig. 1.** Variations of thermophysical properties of water at  $P = 25$  MPa.

abnormal heat transfer phenomenon, either the heat transfer enhancement or the heat transfer deterioration could appear in the upward channels at the supercritical condition [3–6]. When the heat transfer deterioration happens, the heat transfer coefficient is lower, which may lead to higher wall temperatures that might be above the maximum allowable temperature for the cladding surface of the fuel rods. Therefore, an accurate prediction of the wall temperature is very important before the fuel assembly is put into use in the reactor. Thus far, several researchers have made efforts on both the experimental and numerical studies on the fluid flow and heat transfer of the supercritical water in the circular tube [7–17]. The works showed the effects of the buoyancy and the thermal acceleration due to the sharp variations of thermal physical properties of the supercritical water near the pseudo-critical point might be the main reasons of the abnormal heat transfer

phenomenon.

Extensive experimental studies using the supercritical water in the vertical upward tube have been made by several researchers, such as the works by Shen et al. and Pioro [10], [12,13]. Most of the studies focused on the investigation of the heat transfer characteristics or developing the heat transfer correlations at the supercritical conditions. However, there were just a few experimental works for the supercritical water in the upward fuel bundle of the reactor [14], [18–21] until now. In addition to the experimental studies, researchers have performed many numerical studies by the CFD simulations of flow and thermal field in the supercritical water channels [7–10], [22–24]. Most of the CFD studies applied the Reynolds-averaged Navier – Stokes approach. Different turbulent models have been assessed against the available experimental data. The performance of the turbulent models varied case-by-case. It mainly

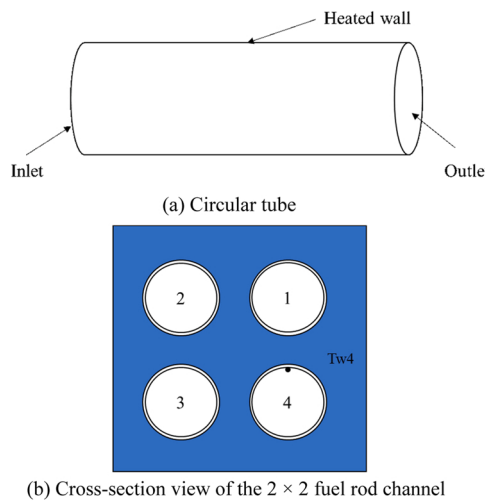


**Fig. 2.** Experimental flow channels used in the study.

depends on the operating conditions, such as the heat to mass flux ratio, the geometry of the flow channel, and the flow direction [14], [25]. Among them, the heat to mass flux ratio plays a dominant role. However, there is no general consensus on the criterion of the heat to mass flux ratio for the onset of the heat transfer deterioration. Due to the limited experimental data under the supercritical conditions, the turbulent Prandtl number was assumed to be a constant in the previous CFD simulations. The dramatic variations of the thermal physical properties near the pseudo-critical point makes the predictive assessment more difficult. The strong buoyancy and thermal acceleration effect caused by the strong variations of the thermophysical properties of the supercritical water near the pseudo-critical point should be considered in the simulations. Most turbulent models used in CFD simulations were developed for incompressible and constant-property flows. For conventional fluids without large variations of thermal physical properties,  $\text{Pr}_t$  can be treated as a constant based on the Reynolds analogy assumption, ranging from 0.8 to 0.9. However, the  $\text{Pr}_t$  changes sharply at supercritical conditions [26–33]. Therefore, an appropriate treatment of the turbulent Prandtl number at the supercritical condition is needed. There are no available experimental data of  $\text{Pr}_t$  for the supercritical fluid now. Several  $\text{Pr}_t$  models have been proposed in literatures. Myong et al. [27] proposed a variable  $\text{Pr}_t$  model for the heat transfer in a fully developed turbulent pipe flow which was heated by a constant heat flux. The fluid used in the numerical simulations were not mentioned. Two  $\text{Pr}_t$  models were put developed by Kays and Crawford [28,29]. The parameters used in the models were derived from the experimental studies on the heat transfer of transformer oil, water, air, but, not under a supercritical condition. Tang et al. [30] introduced a variable  $\text{Pr}_t$  model for the heat transfer of the supercritical carbon dioxide in the upward tube. Kong et al. [31] then assessed the accuracy of Tang et al.'s model for the heat transfer of the supercritical water in the upward tube. The results showed the prediction is not satisfactory. This seems to signify that the difference of the critical parameters may lead to the variations of the turbulent Prandtl number although the heat transfer characteristics of supercritical fluids are similar. Jiang et al. [32] and

Bae [33] developed similar  $\text{Pr}_t$  models for supercritical carbon dioxide and supercritical water in circular tubes. The models were both functions of non-dimensional distance from the wall ( $y^+$ ). After investigating the accuracy of the previous turbulent models, Kong et al. [31] introduced a new variable  $\text{Pr}_t$  model considering the effects of the pressure, turbulent viscosity, and molecular Prandtl number for the heat transfer of the supercritical water in an upward tube. The predictions of the wall temperatures by this model are satisfactory except for deteriorated heat transfer operating conditions where there are still large discrepancies.

The objectives of the present study are (1) to propose a new variable  $\text{Pr}_t$  model for supercritical fluid flows, (2) to find the best existing turbulent models for the prediction of the wall temperature in the supercritical flow channels, and (3) to modify the existing turbulent models using the proposed variable  $\text{Pr}_t$  model.

## 2. Numerical modeling

### 2.1. Configuration of the flow channels

In this work, the experimental data used for the assessment of the simulations of the supercritical water in the upward circular tube and the multiple fuel rods channels are from Mokry et al. [34] and Li [14], respectively. The experimental uncertainties of the wall temperatures for Cases 1–3 are  $\pm 3.0\%$  and Cases 4 – 5 are  $\pm 1.5\text{C}$ . The configurations of these two types of channels are shown in Fig. 2 and the geometrical and operating parameters used in all simulations are listed in Table 1.

### 2.2. Numerical model and governing equations

The numerical simulations are carried out by the commercial software ANSYS FLUENT. The governing equations of the fluid flow and heat transfer of the supercritical water in the channels are the conservation of mass, momentum, and energy. The Reynolds averaged form of the governing equations can be described as [35]:

$$\frac{\partial \bar{u}_i}{\partial x_i} = 0 \quad (1)$$

$$\frac{\partial (\rho \bar{u}_i \bar{u}_j)}{\partial x_j} = -\frac{\partial \bar{p}}{\partial x_i} + \frac{\partial}{\partial x_j} \left( \mu \frac{\partial \bar{u}_i}{\partial x_j} - \rho \bar{u}_i \bar{u}_j \right) \quad (2)$$

$$\frac{\partial}{\partial x_i} (\bar{u}_i \rho c_p T) = \frac{\partial}{\partial x_i} \left[ \left( \lambda + \frac{c_p \mu_t}{\text{Pr}_t} \right) \frac{\partial T}{\partial x_i} \right] \quad (3)$$

Four turbulent models are applied in this study to solve the Reynolds stress term, including the realizable  $k - \varepsilon$  model [34], the RNG (renormalization group)  $k - \varepsilon$  model [34], the  $k - \omega$  SST model [35], and the Reynolds Stress Model [35].

The transport equations for the turbulent kinetic energy ( $k$ ) and the dissipation rate ( $\varepsilon$ ) in the realizable  $k - \varepsilon$  model are given as [35]:

$$\frac{\partial}{\partial x_i} (\rho k u_i) = \frac{\partial}{\partial x_j} \left[ \left( \mu + \frac{\mu_t}{\sigma_k} \right) \frac{\partial k}{\partial x_j} \right] + G_k + G_b - \rho \varepsilon + S_k \quad (4)$$

**Table 1**

Geometrical and operating conditions of difference cases used in the simulations.

Case #	D (mm)	L (m)	P (MPa)	$T_{in}$ (°C)	$G$ (kg/m <sup>2</sup> s)	$q_w$ (kW/m <sup>2</sup> )	$q_w/G$ (kW·s/kg)	Heat transfer condition
1 [34]	10	4	24.1	350	1503	590	0.393	NHT
2 [34]	10	4	23.9	350	1002	681	0.681	NHT
3 [34]	10	4	24.1	350	203	129	0.635	DHT
4 [14]	8	1.328	25	339.6	795.1	1007.6	1.267	NHT
5 [14]	8	1.328	25	340.1	451.2	551.6	1.223	DHT

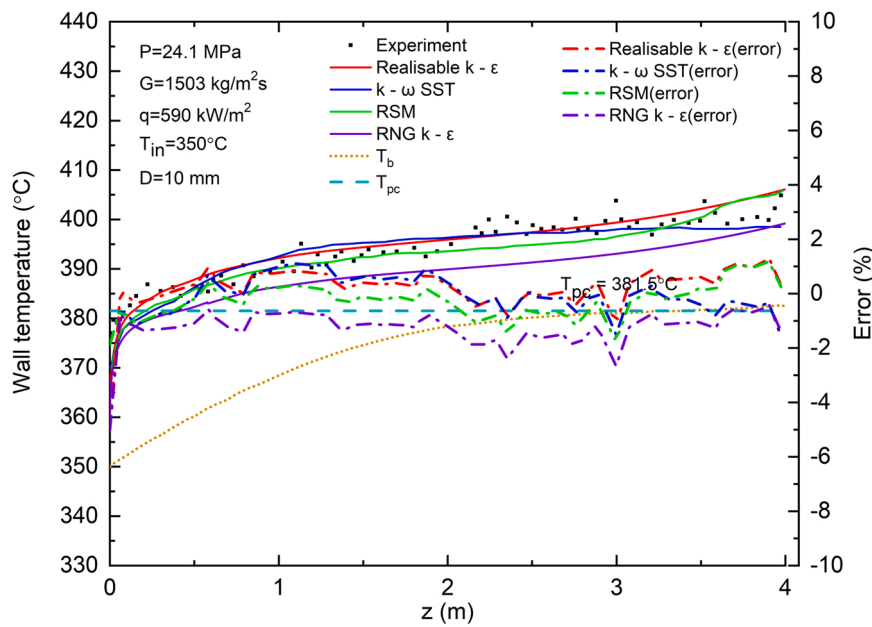


**Fig. 3.** Comparison of the predicted wall temperatures by different turbulence models with the experimental data for Case 1.

$$\frac{\partial}{\partial x_i} (\rho \epsilon u_i) = \frac{\partial}{\partial x_j} \left[ \left( \mu + \frac{\mu_t}{\sigma_\epsilon} \right) \frac{\partial \epsilon}{\partial x_j} \right] + \rho C_1 S \epsilon - \rho C_2 \frac{\epsilon^2}{k + \sqrt{\nu \epsilon}} + C_{1\epsilon} \frac{\epsilon}{k} C_{3\epsilon} G_b + S_\epsilon \quad (5)$$

where,

$G_k$  is the generation of the turbulent kinetic energy.

$G_b$  is the generation of the turbulent kinetic energy due to buoyancy.

$S_k$  and  $S_\epsilon$  are user-defined source terms.

$C_1 = \max [0.43, \frac{\eta}{\eta+5}]$ ,  $\eta = S \frac{k}{\epsilon}$ ,  $S_{ij} = \frac{1}{2} \left( \frac{\partial u_i}{\partial x_j} + \frac{\partial u_j}{\partial x_i} \right)$ .

$C_2$ ,  $C_{1\epsilon}$ ,  $\sigma_k$ , and  $\sigma_\epsilon$  are constants.

For the RNG  $k - \epsilon$  model, the transport equation for  $k$  is the same as that in the realizable  $k - \epsilon$  model while the transport equation for the dissipation rate ( $\epsilon$ ) is different [35]:

$$\frac{\partial}{\partial x_i} (\rho \epsilon u_i) = \frac{\partial}{\partial x_j} \left( \alpha_\epsilon \mu_{eff} \frac{\partial \epsilon}{\partial x_j} \right) + C_{1\epsilon} \frac{\epsilon}{k} (G_k + C_{3\epsilon} G_b) - C_{2\epsilon} \rho \frac{\epsilon^2}{k} - R_\epsilon + S_\epsilon \quad (6)$$

where,  $R_\epsilon = \frac{C_\mu \rho \eta^3 (1 - \eta/\eta_0)}{1 + \beta \eta^3} \frac{\epsilon^2}{k}$ ,  $\eta_0$ ,  $\beta$ ,  $C_\mu$  and  $C_{2\epsilon}$  are constants.

The transport equations for  $k$  and the specific dissipation rate  $\omega$ , which is the rate at which turbulent kinetic energy is converted into thermal internal energy per unit volume and time, in the  $k - \omega$  SST model are expressed as [35]:

$$\frac{\partial}{\partial x_i} (\rho k u_i) = \frac{\partial}{\partial x_j} \left( \left( \mu + \frac{\mu_t}{\sigma_k} \right) \frac{\partial k}{\partial x_j} \right) + \widetilde{G}_k - Y_k + S_k \quad (7)$$

$$\frac{\partial}{\partial x_i} (\rho \omega u_i) = \frac{\partial}{\partial x_j} \left( \left( \mu + \frac{\mu_t}{\sigma_\omega} \right) \frac{\partial \omega}{\partial x_j} \right) + \widetilde{G}_\omega - Y_\omega + D_\omega + S_\omega \quad (8)$$

where,

$\widetilde{G}_k$  and  $\widetilde{G}_\omega$  are the generations of  $k$  and  $\omega$ , respectively.

$Y_k$  and  $Y_\omega$  are the dissipations of  $k$  &  $\omega$  due to turbulence.

$D_\omega$  is the cross-diffusion term.

As for the Reynolds stress model, the transport equation can be written as [34]:

$$\begin{aligned} \frac{\partial}{\partial x_k} (\rho u_k \bar{u}_i \bar{u}_j) &= - \underbrace{\frac{\partial}{\partial x_k} \left[ \rho \bar{u}_i \bar{u}_j \bar{u}_k + p' (\delta_{kj} \bar{u}_i + \delta_{ik} \bar{u}_j) \right]}_{C_{ij} \equiv \text{Convection}} + \\ &\underbrace{\frac{\partial}{\partial x_k} \left[ \mu \frac{\partial}{\partial x_k} (\bar{u}_i \bar{u}_j) \right]}_{D_{L,ij} \equiv \text{Molecular Diffusion}} - \underbrace{\rho \left( \bar{u}_i \bar{u}_k \frac{\partial u_j}{\partial x_k} + \bar{u}_j \bar{u}_k \frac{\partial u_i}{\partial x_k} \right)}_{P_{ij} \equiv \text{Stress Production}} - \underbrace{\rho \beta (g_i \bar{u}_j \theta + g_j \bar{u}_i \theta)}_{G_{ij} \equiv \text{Buoyancy Production}} + \\ &\underbrace{p' \left( \frac{\partial \bar{u}_i}{\partial x_j} + \frac{\partial \bar{u}_j}{\partial x_i} \right)}_{\phi_{ij} \equiv \text{Pressure Strain}} - 2 \underbrace{\mu \frac{\partial \bar{u}_i \bar{u}_j}{\partial x_k \partial x_k}}_{\varepsilon_{ij} \equiv \text{Dissipation}} - 2 \rho \Omega_k (\bar{u}_j \bar{u}_m \varepsilon_{ikm} + \bar{u}_i \bar{u}_m \varepsilon_{jkm}) + \underbrace{S_{user}}_{F_{ij} \equiv \text{Production by System Rotation}} \end{aligned} \quad (9)$$

The modeling of the above terms is explained detail in [35].

In the numerical simulations, the mesh near the wall in the radial direction is refined until  $y^+ \approx 1$  at the first node from the wall so that the enhanced wall treatment method can be applied. The thermophysical properties of supercritical water from the NIST standard REFPROP database 9.1 [2] were implemented into Fluent by using piecewise-linear function of temperature. The SIMPLEC solution algorithm is used for the pressure-velocity coupling and the QUICK method is used for the spatial discretization in the simulations. The grid independent tests were also performed for each geometry in the simulations. In all the simulations of the present work, the heat flux applied on the walls are assumed constant and uniform. The thermal physical properties of the supercritical water are from [4].

### 3. Evaluation of standard turbulent models

Five experimental cases are selected in the study to assess the performance of different turbulent models, among them Cases 1–3 are for the flows in an upward circular tube and Cases 4–5 are for flows in upward multiple fuel rods channels. Since an accurate wall temperature prediction of the fuel rod in the reactor is significant for the design and safety of the SCWR, the wall temperatures are compared with the experimental data in the present work.

#### 3.1. Flows in the upward circular tube

The comparisons of the numerical results for the wall temperatures with different turbulent models and the experimental data as well as the

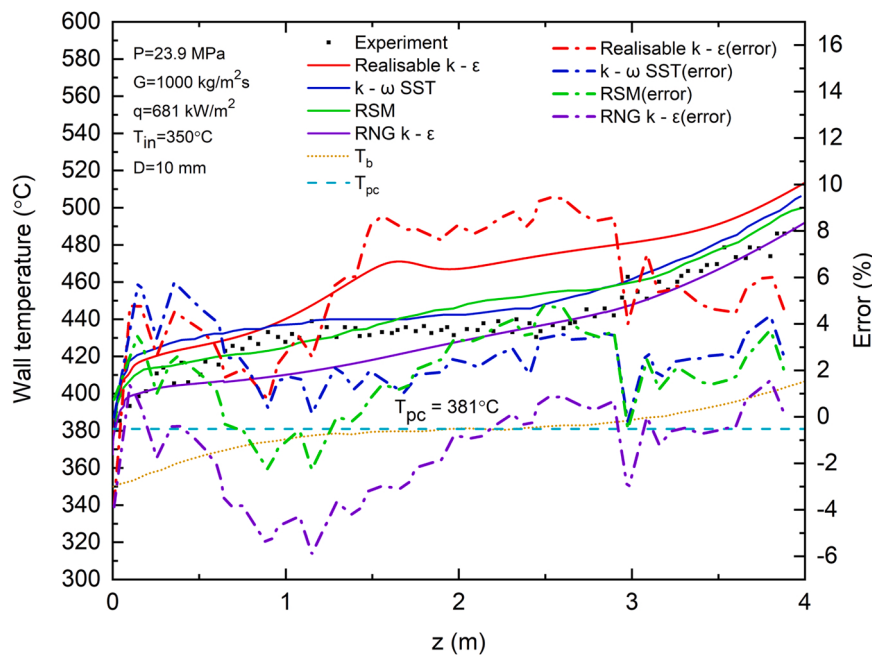


Fig. 4. Comparison of the predicted wall temperatures by different turbulence models with the experimental data for Case 2.

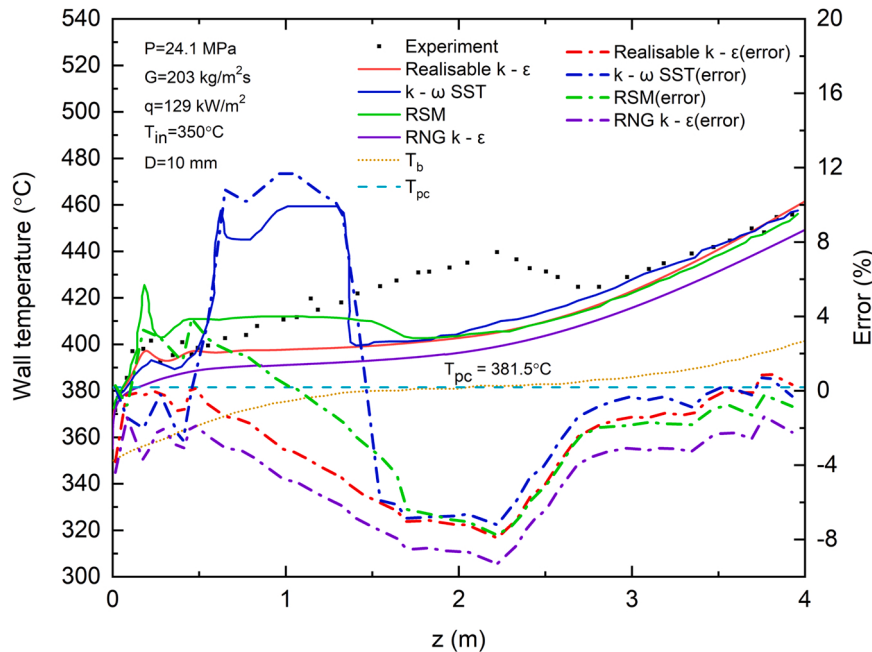
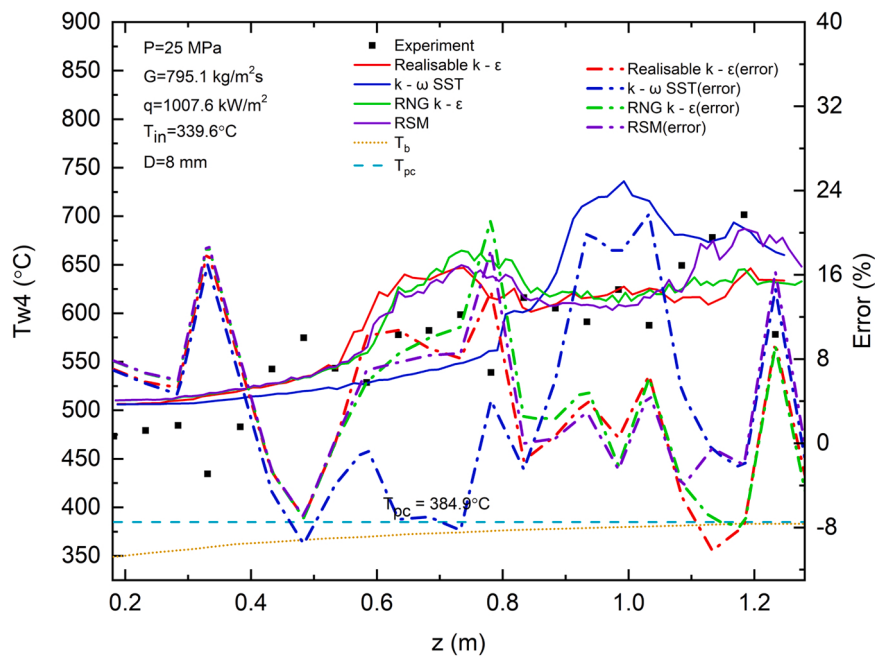


Fig. 5. Comparison of the predicted wall temperatures by different turbulence models with the experimental data for Case 3.

relative errors are presented in Figs. 3 – 5.

It is obvious that most of the selected turbulent models can predict the wall temperature variations from the entrance to the exit of the circular tube reasonably well in Cases 1 and 2 except that the Realisable  $k - \varepsilon$  model overpredicts the wall temperatures in Case 2. In Case 3, the Realisable  $k - \varepsilon$  model and  $k - \omega$  SST model show a good agreement with the experimental data in the entrance region ( $z = 0 - 0.5 \text{ m}$ ), while all selected turbulent models except for the RNG  $k - \varepsilon$  model behave well near the exit region ( $z = 3 - 4 \text{ m}$ ). None of the turbulent models can give good predictions for the wall temperature in the middle region of the tube ( $z = 0.5 - 3 \text{ m}$ ) where the experimental wall temperature increases along the  $x$  direction and reaches a peak value at  $z = 2.25 \text{ m}$ , however, all models cannot predict a peak temperature in this region and the

predicted wall temperatures are much lower than the experimental data. The RNG  $k - \varepsilon$  model predicts the lowest the wall temperature compared with other models. Other three turbulent models could capture the wall temperature variations near the exit ( $z = 3 - 4 \text{ m}$ ) quite well. Both the  $k - \omega$  SST model and RSM show a drastic wall temperature increase near the inlet, which does not agree with the experimental data. Cases 1 and 3 have the same operating pressure and the inlet temperature, but different heat to mass flux ratios. However, the selected turbulent models at the high heat to mass flux ratio condition (Case 3) cannot predict the wall temperature distribution as well as that at the low heat to mass flux ratio condition (Case 1). For the cases with the same inlet temperature and similar heat to mass flux ratio (Cases 2 and 3), the deviations between the predicted results by different turbulent models



**Fig. 6.** Comparison of the predicted wall temperatures by different turbulence models with the experimental data for Case 4.

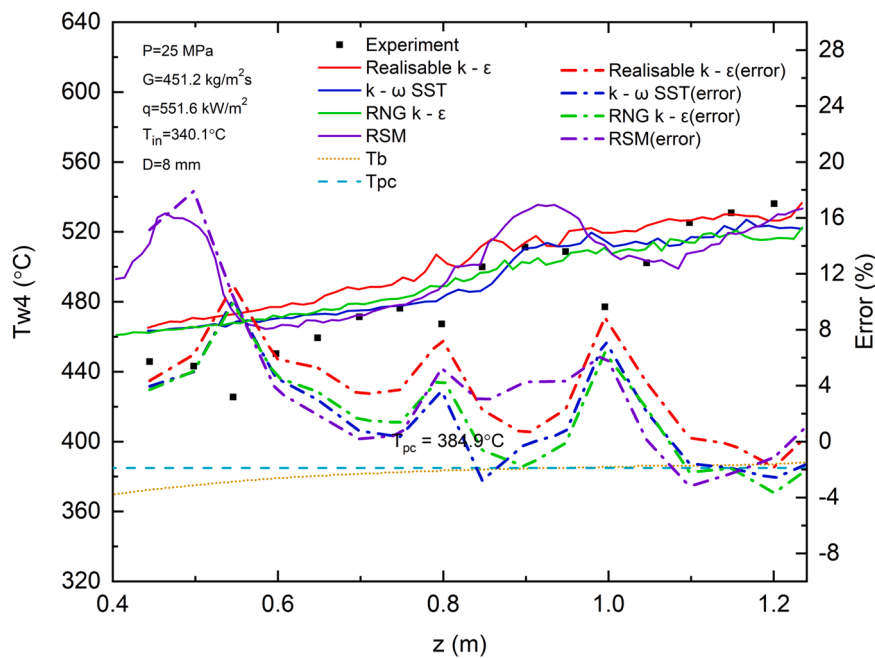


**Fig. 7.** Comparison of the predicted wall temperatures by different turbulence models with the experimental data for Case 5.

and the experimental data become larger at the lower mass flux condition (Case 3) where heat transfer deterioration happens.

### 3.2. Flows in upward $2 \times 2$ fuel rod channel

Figs. 6 and 7 show the comparison of the predicted wall temperatures using different turbulent models for the  $2 \times 2$  fuel rod channel with the experimental data. The sudden drop and then sharp increase in the wall temperature near the entrance observed in the experimental data in Case 4 are not predicted by any of the turbulent models as shown in Fig. 6. For Case 4, the  $k - \omega$  SST model underestimates the wall temperatures in the region  $z = 0.6\text{--}0.8$  m while other turbulent models overpredict the wall temperatures. In the region  $z = 0.8\text{--}1.1$  m, all models behave well

except the  $k - \omega$  SST model gives much higher wall temperature than the experimental data. The Reynolds stress model performs quite well both qualitatively and quantitatively while both the RNG and Realizable  $k - \varepsilon$  models predict lower wall temperatures than the experimental data in the region  $z = 1.1\text{--}1.2$  m. For Case 5, the RSM gives much higher wall temperatures than the experimental data in the region  $z = 0.4\text{--}0.6$  m. All other three turbulent models cannot predict the wall temperature drop in the region  $z = 0.4\text{--}0.6$  m, which was observed in the experimental data. However, they all can capture the wall temperature distributions well in the region  $0.6\text{--}1.2$  m, except for the sudden wall temperature drop at  $z = 1.0$  m as shown in the experimental data. In addition, the RSM generally gives a high wall temperature prediction, but it can reproduce the drop and increase trend of the wall temperature

**Table 2**

Relative errors between the numerical and experimental results for the wall temperature.

Case#	$RE = \left  \frac{T_{w,num} - T_{w,exp}}{T_{w,exp}} \right  \times 100\%$									
Model	Realisable $k - \varepsilon$		RNG $k - \varepsilon$		$k - \omega$ SST		RSM		Average	
Error (%)	MAE	SD	MAE	SD	MAE	SD	MAE	SD	MAE	SD
<b>Single tube</b>										
1	0.55	0.65	1.38	0.66	0.34	0.44	0.35	0.40	0.66	0.54
2	5.44	2.56	1.94	1.63	1.56	0.75	1.22	1.06	2.54	1.5
3	2.80	2.51	4.44	2.43	2.39	3.32	1.70	2.04	2.83	2.58
<b>Average_ Single tube</b>	2.93	1.91	2.59	1.57	<b>1.43</b>	1.50	<b>1.09</b>	<b>1.17</b>	2.01	1.54
<b>Tube bundle</b>										
4	6.34	4.36	9.28	7.25	8.96	5.63	6.57	5.26	7.79	5.63
5	4.01	3.15	3.39	2.47	3.07	2.66	4.75	5.28	3.81	3.39
<b>Average_ Tube bundle</b>	<b>5.18</b>	<b>3.76</b>	6.34	4.86	6.02	<b>4.15</b>	5.66	5.27	5.8	4.51
<b>Average</b>	3.83	2.65	4.09	2.89	3.26	<b>2.56</b>	<b>2.92</b>	2.81	3.53	2.73

MAE - Mean of Absolute Error; SD - Standard Deviation; RE – Relative Error

near  $z = 1.0$  m, which was observed in the experimental data.

Table 2 shows the relative errors between the numerical and experimental wall temperatures for all the cases mentioned above. It can be seen that the errors of the predicted results for Cases 4 and 5 are higher than Cases 1–3. This might attribute the complexity of the flow in a shield side of a tube bundle than the internal flow in a tube. The flows in such tightly packed nuclear reactor rod bundle have unique regimes, which not appear in the tube flow in simple channels [36,37]. Strong transverse and large - scale motions could be observed in the narrow gaps between the neighbouring fuel rods or between a fuel rod and the surrounding adiabatic walls [8], [20–23]. The heat and turbulence transfer in the near rod region, especially in the boundary layer, may not be accurately predicted by the conventional turbulent models. Among all cases, the average error from the RNG  $k - \varepsilon$  model is higher than the other three turbulent models. Therefore, the Realisable  $k - \varepsilon$  model,  $k - \omega$  SST model and the Reynolds stress model will be modified further to improve the performance.

#### 4. Modified turbulent models

##### 4.1. Turbulent Prandtl number

The discrepancies between the numerical results and the experimental data for supercritical fluid flow and heat transfer can be due to the improper treatment of the momentum and heat eddy diffusivity at the supercritical conditions. The turbulent Prandtl number used in the governing equations is a non-dimensional parameter which measures the relationship of the momentum eddy diffusivity and the heat transfer eddy diffusivity. It can be defined as:

$$\text{Pr}_t = \frac{v_t}{\alpha_t} = \frac{\mu_t/\rho}{\lambda_t/(\rho c_p)} = \frac{\mu_t c_p}{\lambda_t} \quad (10)$$

In the energy equation, Eq. (3), the diffusion can be rearranged as:

$$\begin{aligned} \frac{\partial}{\partial x_i} \left[ \left( \lambda + \frac{c_p \mu_t}{\text{Pr}_t} \right) \frac{\partial T}{\partial x_i} \right] &= \frac{\partial}{\partial x_i} \left[ \left( \frac{\lambda}{c_p} + \frac{\lambda_t}{c_p} \right) \frac{\partial h}{\partial x_i} \right] \\ &= \frac{\partial}{\partial x_i} \left[ \mu \left( \frac{1}{\text{Pr}} + \frac{\mu_t/\mu}{\text{Pr}_t} \right) \frac{\partial h}{\partial x_i} \right] \end{aligned} \quad (11)$$

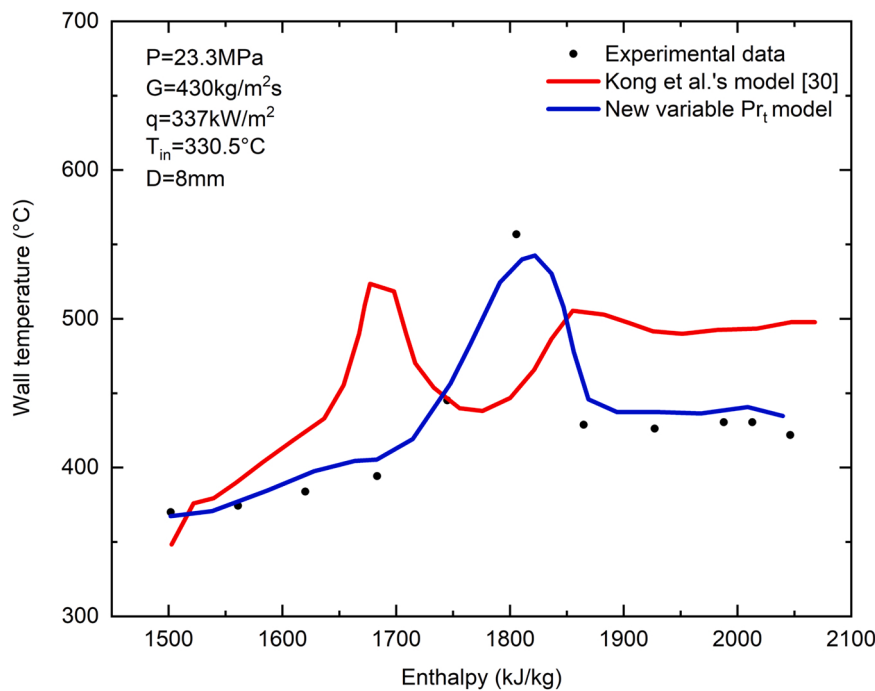
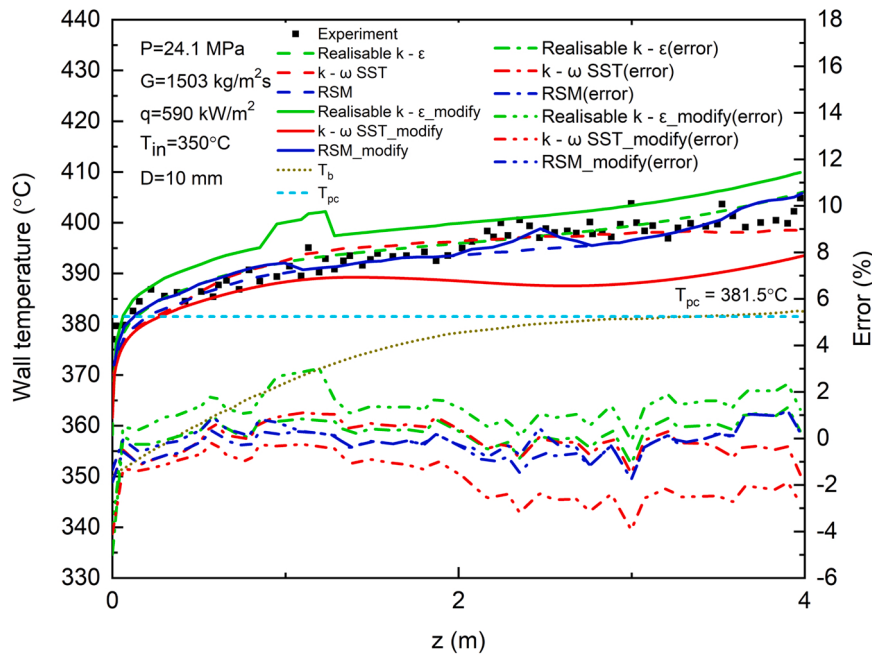


Fig. 8. Comparison the predicted wall temperatures using the proposed model with the results using Kong's model [31] and the experimental data [39].



**Fig. 9.** Comparison of the predicted wall temperatures by the original and modified turbulence models with the experimental data for Case 1.

Thus, the heat transfer is influenced by both  $\text{Pr}$  and  $\text{Pr}_t$ . The term  $\frac{1}{\text{Pr}}$  stands for the heat transfer contributed by the molecular conduction and the term  $\frac{\mu/\mu_t}{\text{Pr}_t}$  represents the heat transfer contributed by the turbulent mixing. Thus, it can be concluded that the heat transfer contributed by the turbulent mixing will increase if the turbulent Prandtl number decreases.

For the flow in the near wall region, especially in the viscous sublayer, it is known that  $\mu_t/\mu \ll 1$ . The molecular conduction plays a dominant role in the heat transfer [38]. Similarly, the heat transfer contributed by the turbulent mixing dominates in the high Reynolds number core flow region since  $\mu_t/\mu \gg 1$ . However, in the buffer layer near the wall region, where  $\mu_t/\mu \approx 1$ , the heat transfer contributions by the molecular conduction and turbulent mixing are in the same

magnitude. Thus, it is necessary to determine the  $\text{Pr}_t$  realistically, so that the heat transfer contributions can be accurately predicted.

$\text{Pr}_t$  is commonly assumed as a constant, 0.85 or 0.9 in the existing turbulent models, whose value was based on the experimental or direct numerical simulations for common fluids. This is generally accurate for fully developed turbulent flow. However, the thermal physical properties of the supercritical fluid vary sharply near the pseudo-critical region. It is irrational to still assume  $\text{Pr}_t$  as a constant under the supercritical condition, especially if the fluid undergoes the dramatic variations of properties in the buffer layer. There is no experimental data of  $\text{Pr}_t$  for the supercritical water to date. Most of the proposed  $\text{Pr}_t$  models for the supercritical fluids in the previous studies [30–33] are for the supercritical carbon dioxide in the tube flow. The  $\text{Pr}_t$  model proposed

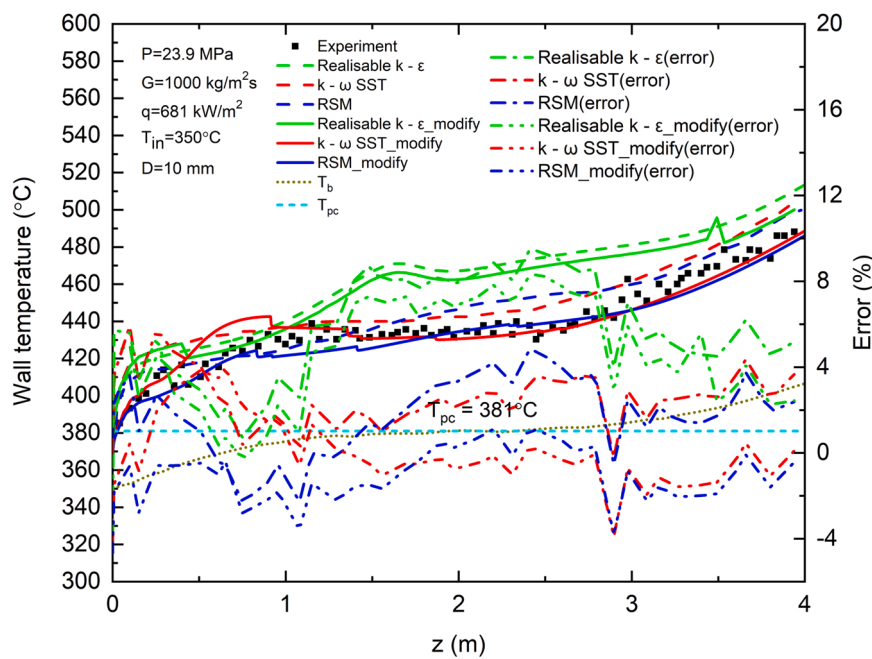


**Fig. 10.** Comparison of the predicted wall temperatures by the original and modified turbulence models with the experimental data for Case 2.

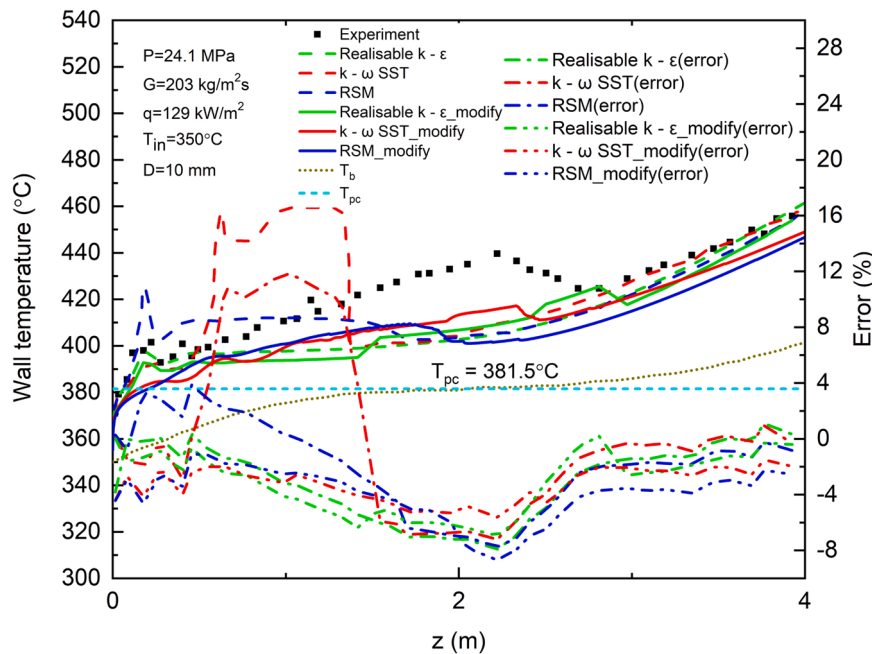


Fig. 11. Comparison of the predicted wall temperatures by the original and modified turbulence models with the experimental data for Case 3.

by Kong et al. [31] was for the supercritical water flow and heat transfer inside a tube. They assessed the existing turbulent Prandtl models in their study and then compared the performance of their proposed model with the existing models. Generally, the  $\text{Pr}_t$  model proposed by Kong et al. achieved better prediction accuracy than the existing models. Thus, Kong et al.'s  $\text{Pr}_t$  model is selected here to be modified further for the supercritical water flow and heat transfer in rod bundles. The Kong et al.'s model is given as:

$$\text{Pr}_t = \begin{cases} 0.3 + 0.03 \times (P/P_{cr}) \times \text{Pr} & \mu_t/\mu < 0.2 \\ 0.4 & 0.2 \leq \mu_t/\mu \leq 10 \\ 0.85 & \mu_t/\mu > 10 \end{cases} \quad (12)$$

Number of researchers pointed out that the heat to mass flux ratio may be the key factor that affects the heat transfer phenomenon [7,8,10, 11,15–19]. Thus, a new variable  $\text{Pr}_t$  model based on Kong et al.'s model is developed in this study as below:

$$\text{Pr}_t = \begin{cases} 0.4 & \mu_t/\mu < 0.2 \\ 0.3 + 0.03 \times (P/P_{cr}) \times \text{Pr} \times (\mu_t/\mu) \times (q/G) & 0.2 \leq \mu_t/\mu \leq 10 \\ 0.85 & \mu_t/\mu > 10 \end{cases} \quad (13)$$

The proposed turbulent model with the variable  $\text{Pr}_t$  model given in Eq. (13) will be assessed first by comparing the predictions of the wall temperatures with the experimental data for the case with a heat transfer deterioration in a tube flow [39], which was used in the study by

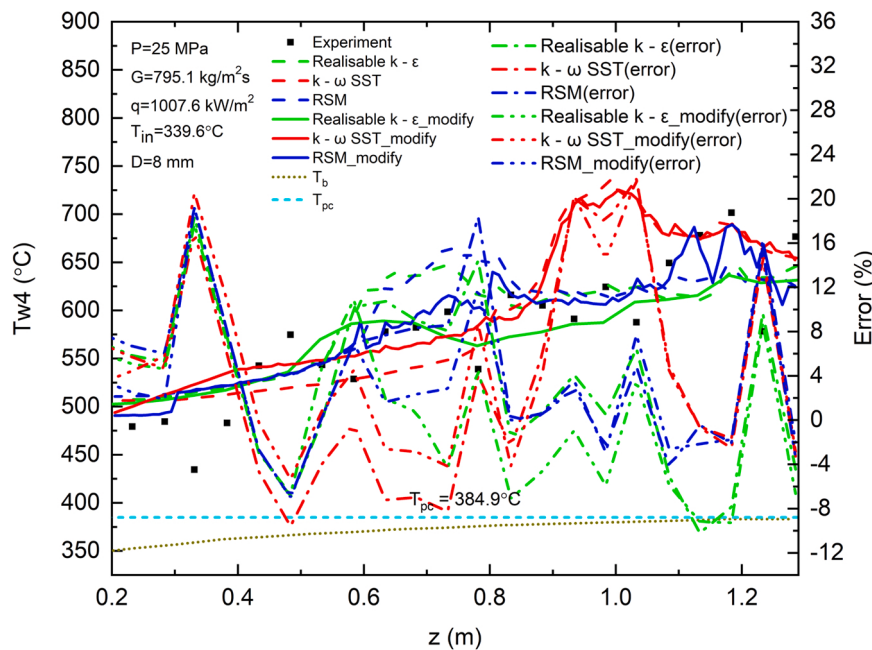
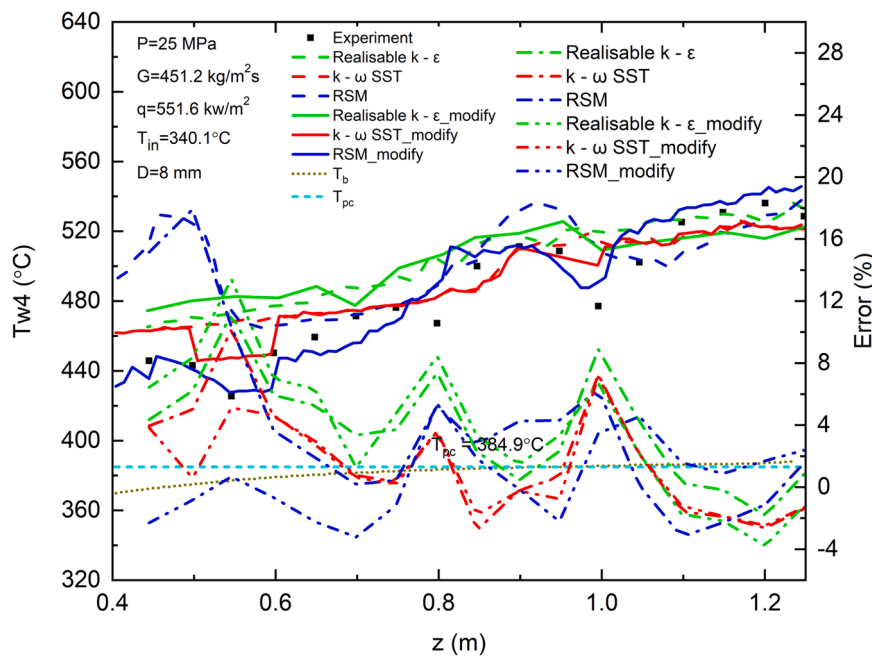


Fig. 12. Comparison of the predicted wall temperatures by the original and modified turbulence models with the experimental data for Case 4.



**Fig. 13.** Comparison of the predicted wall temperatures by the original and modified turbulence models with the experimental data for Case 5.

**Table 3**

Relative errors between the numerical and experimental results for the wall temperatures.

Case#	$RE = \left( \frac{T_{w,num} - T_{w,exp}}{T_{w,exp}} \right) \times 100\%$							
Model	Realisable_modified		SST_modified		RSM_modified		Average	
Error (%)	MAE	SD	MAE	SD	MAE	SD	MAE	SD
<b>Single tube</b>								
1	1.33	0.72	1.79	0.99	0.31	0.28	1.14	0.66
2	4.54	2.45	1.25	1.11	1.27	0.85	2.35	1.47
3	3.01	2.10	3.09	1.26	3.62	1.93	3.24	1.76
<b>Average_Single tube</b>	2.96	1.76	2.04	1.12	1.73	1.02	2.24	1.30
<b>Tube bundle</b>								
4	6.05	3.62	7.17	6.60	4.60	5.04	5.94	5.09
5	4.81	3.34	1.95	1.59	1.88	1.24	2.88	2.06
<b>Average_Tube bundle</b>	5.43	3.48	4.56	4.10	3.24	3.14	4.41	3.58
<b>Average</b>	3.95	2.45	3.05	2.31	2.34	1.87	3.11	2.21

Kong et al. [31], as well as the numerical results from Kong et al. [31]. Since  $k - \omega$  SST model was used in the work by Kong et al. [31], it is also used here for the comparison purpose. Fig. 8 presents the comparison of the predicted wall temperature distributions using the proposed variable  $\Pr_t$  model with the experimental data [39] and the numerical results from Kong et al. [31]. It can be seen that the numerical results using the proposed  $\Pr_t$  model gives much better prediction than the results from the  $\Pr_t$  model by Kong et al.'s [31] compared with the experimental data as shown in Fig. 8. However, this is just for one low heat flux and low mass flux tube flow case ( $q_w/G = 0.784$ ). Therefore, the performance of the proposed variable  $\Pr_t$  model will also be assessed under different operating conditions of tube flows and the fuel rod channel flows as well as for other turbulent models. Thus, the proposed variable  $\Pr_t$  model is used with the Realisable  $k - \epsilon$  model, the  $k - \omega$  SST model and the Reynolds Stress model to simulate the fluid flow and heat transfer of the supercritical water in both the upward flows in tubes and the channel with multiple fuel rods.

#### 4.2. Results and discussions

The five cases listed in Table 1 are applied here to evaluate the performance of the modified turbulent models. Figs. 9 – 11 are the

comparisons between the numerical results by the original and modified turbulent models and the experimental results for the upward circular tube (Cases 1 – 3). Figs. 12 – 13 are the comparisons for the upward  $2 \times 2$  fuel rod channel (Cases 4 – 5). The relative errors between the numerical and experimental results are presented in Table 3.

It is obvious that the modified Reynolds stress model shows a great improvement on the predictions of the wall temperature and could predict the general trend of the wall temperatures well in all cases. However, it should be noted that all the modified turbulent models still underpredict the wall temperature at the center region in Case 3. For the multiple fuel rods channel, although the modified RSM can predict the wall temperature reasonably well, there are some fluctuations in the wall temperatures at the exit region in Case 4. The modified RSM gives the best agreement with the experimental data compared with other turbulent models.

#### 5. Conclusions

In this study, a new variable  $\Pr_t$  model is developed, and modified Realisable  $k - \epsilon$  model, the  $k - \omega$  SST model and the RSM are proposed using the new variable  $\Pr_t$  to improve the performance of the numerical models for supercritical fluid flow and heat transfer. The assessment of

the proposed turbulent models was carried out for the supercritical water flows in both the upward circular tube and the upward channel with multiple fuel rods. The wall temperatures predicted by the modified Realisable  $k - \epsilon$  model, the  $k - \omega$  SST model and the RSM with the new variable  $\text{Pr}_t$  are strongly improved compared with the standard Realisable  $k - \epsilon$  model, the  $k - \omega$  SST model and the RSM. The modified RSM gives the best agreement with the experimental data than other modified turbulent models. The future work will focus on improving the modified RSM quantitatively through the calibrations of the constants used in the model with more experimental data at various operating conditions when they are available.

## Declaration of Competing Interest

The authors declare that they have no known competing financial interests or personal relationships that could have appeared to influence the work reported in this paper.

## Acknowledgements

This work was supported by the Natural Sciences and Engineering Research Council of Canada (NSERC) Discovery grant [grant number #04757].

## References

- [1] GIF, 2018. "GIF R&D Outlook for Generation IV Nuclear Energy Systems 2018 Update," *Nuclear Energy*, 2018.
- [2] Lemmon E., Huber M., McLinden M., 2013. NIST reference fluid thermodynamic and transport properties-RFFPROP, version 9.1. National Institute of Standard Technology. 2013.
- [3] I.L. Pioro (Ed.), *Handbook of Generation IV Nuclear Reactors*, First ed., Elsevier—Woodhead Publishing, Duxford, UK, 2016.
- [4] I. Pioro, S. Mokry, Thermophysical Properties at Critical and Supercritical Pressures. Heat Transfer - Theoretical Analysis, Experimental Investigations and Industrial Systems, In Tech Open Science, 2011, pp. 573–592.
- [5] I. Pioro, S. Mokry, S. Draper, Specifics of thermophysical properties and forced-convective heat transfer at critical and supercritical pressures, *Rev. Chem. Eng.* (2011), <https://doi.org/10.1515/REVCE.2011.501>.
- [6] S.J. Mokry, P.L. Kirillov, I.L. Pioro, Y.K. Gospodinov, Supercritical Water Heat Transfer in a Vertical Bare Tube: Normal, Improved, and Deteriorated Regimes, *Nucl. Technol.* 172 (1) (2010) 60–70. (<https://doi.org/10.13182/nt10-a10882>).
- [7] S. Koshizuka, N. Takano, Y. Oka, Numerical analysis of deterioration phenomena in heat transfer to supercritical water, *Int. J. Heat. Mass Transf.* vol. 38 (16) (1995) 3077–3084. ([https://doi.org/10.1016/0017-9310\(95\)00008-W](https://doi.org/10.1016/0017-9310(95)00008-W)).
- [8] B. Zhang, J. Shan, J. Jiang, Numerical analysis of supercritical water heat transfer in horizontal circular tube, *Prog. Nucl. Energy* 52 (7) (2010) 678–684, <https://doi.org/10.1016/j.pnucene.2010.03.006>.
- [9] X. Cheng, B. Kuang, Y.H. Yang, Numerical analysis of heat transfer in supercritical water-cooled flow channels, *Nucl. Eng. Des.* 237 (3) (2007) 240–252, <https://doi.org/10.1016/j.nucengdes.2006.06.011>.
- [10] Z. Shen, D. Yang, S. Wang, W. Wang, Y. Li, Experimental and numerical analysis of heat transfer to water at supercritical pressures, *Int. J. Heat. Mass Transf.* 108 (2017) 1676–1688, <https://doi.org/10.1016/j.ijheatmasstransfer.2016.12.081>.
- [11] Q.L. Wen, H.Y. Gu, Numerical simulation of heat transfer deterioration phenomenon in supercritical water through vertical tube, *Ann. Nucl. Energy* 37 (10) (2010) 1272–1280, <https://doi.org/10.1016/j.anucene.2010.05.022>.
- [12] G. Zhang, H. Zhang, H. Gu, Y. Yang, X. Cheng, Experimental and numerical investigation of turbulent convective heat transfer deterioration of supercritical water in vertical tube, *Nucl. Eng. Des.* 248 (2012) 226–237, <https://doi.org/10.1016/J.NUCENGDES.2012.03.026>.
- [13] I.L. Pioro, R.B. Duffey, Experimental heat transfer in supercritical water flowing inside channels (furnaces), *Nucl. Eng. Des.* 235 (22) (2005) 2407–2430, <https://doi.org/10.1016/j.nucengdes.2005.05.034>.
- [14] H. Li, M. Zhao, Z. Hu, Y. Zhang, F. Wang, Experimental study of supercritical water heat transfer deteriorations in different channels, *Ann. Nucl. Energy* 119 (2018) 240–256, <https://doi.org/10.1016/j.anucene.2018.05.009>.
- [15] S.Q. Yu, H.X. Li, X.L. Lei, Y.C. Feng, Y.F. Zhang, H. He, T. Wang, Experimental investigation on heat transfer characteristics of supercritical pressure water in a horizontal tube, *Exp. Therm. Fluid Sci.* vol. 50 (2013) 213–221, <https://doi.org/10.1016/j.expthermflusci.2013.06.011>.
- [16] H.Y. Gu, M. Zhao, X. Cheng, Experimental studies on heat transfer to supercritical water in circular tubes at high heat fluxes, *Exp. Therm. Fluid Sci.* (2015), <https://doi.org/10.1016/j.expthermflusci.2015.03.001>.
- [17] K. Yamagata, K. Nishikawa, S. Hasegawa, T. Fujii, S. Yoshida, Forced convective heat transfer to supercritical water flowing in tubes, *Int. J. Heat. Mass Transf.* 15 (1972) 2575–2593. ([https://doi.org/10.1016/0017-9310\(72\)90148-2](https://doi.org/10.1016/0017-9310(72)90148-2)).
- [18] M. Zhao, H.Y. Gu, Experimental and numerical investigation on heat transfer of supercritical water flowing upward in  $2 \times 2$  rod bundles, *Nucl. Eng. Des.* 370 (October) (2020), <https://doi.org/10.1016/j.nucengdes.2020.110903>.
- [19] X. Feng, T. Zhou, J.L. Zhang, B.Y. Zhang, D.L. Ma, Research on heat transfer coefficient of supercritical water based on factorial and correspondence analysis, *Nucl. Eng. Technol.* 52 (7) (2020) 1409–1416, <https://doi.org/10.1016/j.net.2019.12.017>.
- [20] F. Bertocchi, M. Rohde, D. De Santis, A. Shams, H. Dolfen, J. Degroote, J. Vierendeels, Fluid-structure interaction of a 7-rods bundle: benchmarking numerical simulations with experimental data, *Nucl. Eng. Des.* vol. 356 (2020), 110394, <https://doi.org/10.1016/j.nucengdes.2019.110394>.
- [21] M. Bruschewski, M.H.A. Piro, C. Tropea, S. Grundmann, Fluid flow in a diametrically expanded CANDU fuel channel – Part 1: experimental study, *Nucl. Eng. Des.* (September) (2019), 110371, <https://doi.org/10.1016/j.nucengdes.2019.110371>.
- [22] Z. Shang, S. Lo, Numerical investigation of supercritical water-cooled nuclear reactor in horizontal rod bundles, *Nucl. Eng. Des.* 240 (4) (2010) 776–782, <https://doi.org/10.1016/j.nucengdes.2009.10.029>.
- [23] Z. Shen, D. Yang, S. Wang, W. Wang, Y. Li, Experimental and numerical analysis of heat transfer to water at supercritical pressures, *Int. J. Heat. Mass Transf.* 108 (2017), <https://doi.org/10.1016/j.ijheatmasstransfer.2016.12.081>.
- [24] Y. Zhang, C. Zhang, J. Jiang, Numerical simulation of fluid flow and heat transfer of supercritical fluids in fuel bundles, *J. Nucl. Sci. Technol.* 48 (6) (2011) 929–935, <https://doi.org/10.3327/jnst.48.929>.
- [25] X. Lei, H. Li, W. Zhang, N.T. Dinh, Y. Guo, S. Yu, Experimental study on the difference of heat transfer characteristics between vertical and horizontal flows of supercritical pressure water, *Appl. Therm. Eng.* 113 (2017) 609–620, <https://doi.org/10.1016/j.applthermaleng.2016.11.051>.
- [26] X. Chai, X. Liu, J. Xiong, X. Cheng, Numerical investigation of turbulent heat transfer properties at low prandtl number, *Front. Energy Res.* 8 (July) (2020) 1–11, <https://doi.org/10.3389/fenrg.2020.00112>.
- [27] H.K. Myong, N. Kasagi, M. Hirata, Numerical prediction of turbulent pipe flow heat transfer for various prandtl number fluids with the improved k-epsilon turbulence model, *JSME Int. J. Ser. 2* 32 (4) (1989) 613–622. *Fluids Eng. heat Transf. power, Combust. Thermophys.*, (<https://doi.org/10.1299/jsmeb1988.32.4.613>).
- [28] W.M. Kays, 1994. "Turbulent Prandtl Number - Where Are We?", May, 1994.
- [29] W.M. Kays. *Convective Heat and Mass Transfer*, Fourth ed., McGraw-Hill Higher Education., Boston, 2005.
- [30] R. Tian, X. Dai, D. Wang, L. Shi, Study of variable turbulent prandtl number model for heat transfer to supercritical fluids in vertical tubes, *J. Therm. Sci.* 27 (3) (2018) 213–222, <https://doi.org/10.1007/s11630-018-1002-7>.
- [31] X.F. Kong, D. Sun, L. Gou, S. Wang, N. Yang, Numerical investigation on heat transfer of supercritical water with a variable turbulent prandtl number model, *J. Nucl. Eng. Radiat. Sci.* 6 (3) (2020) 1–10, <https://doi.org/10.1115/1.4046025>.
- [32] P.X. Jiang, Z.C. Wang, R.N. Xu, A modified buoyancy effect correction method on turbulent convection heat transfer of supercritical pressure fluid based on RANS model, *Int. J. Heat. Mass Transf.* 127 (2018) 257–267, <https://doi.org/10.1016/J.IJHEATMASSTRANSFER.2018.07.042>.
- [33] Y.Y. Bae, A new formulation of variable turbulent Prandtl number for heat transfer to supercritical fluids, *Int. J. Heat. Mass Transf.* 92 (2016) 792–806, <https://doi.org/10.1016/J.IJHEATMASSTRANSFER.2015.09.039>.
- [34] S. Mokry, I. Pioro, A. Farah, K. King, S. Gupta, W. Peiman, P. Kirillov, Development of supercritical water heat-transfer correlation for vertical bare tubes, *Nucl. Eng. Des.* 241 (4) (2011) 1126–1136, <https://doi.org/10.1016/j.nucengdes.2010.06.012>.
- [35] Ansys. Inc, 2011. "14.0 ANSYS FLUENT Theory Guide," 2011.
- [36] S. Tavoularis, Rod bundle vortex networks, gap vortex streets, and gap instability: A nomenclature and some comments on available methodologies, *Nucl. Eng. Des.* vol. 241 (7) (2011) 2624–2626, <https://doi.org/10.1016/j.nucengdes.2011.03.052>.
- [37] A. Kraus, E. Merzari, T. Norddine, O. Marin, S. Benhamadouche, Direct numerical simulation of fluid flow in a  $5 \times 5$  square rod bundle, *Int. J. Heat. Fluid Flow.* vol. 90 (2021), 108833, <https://doi.org/10.1016/j.ijheatfluidflow.2021.108833>.
- [38] H. Schlichting, K. Gersten. *Boundary-Layer Theory*, Nineth ed., Springer Berlin / Heidelberg, Berlin, Heidelberg, 2016.
- [39] M.E. Shitsman, Impairment of the heat transmission at supercritical pressures(heat transfer process examined during forced motion of water at supercritical pressures), *High. Temp. Sci.* 1 (1963) 237–244.